www.pnas.org/cgi/doi/10.1073/pnas.1918944117

PNAS
www.pnas.org

Supplementary Information for

Non-classical nuclear localization signals mediate nuclear import of CIRBP

Benjamin Bourgeois[1†], Saskia Hutten[2†], Benjamin Gottschalk[1], Mario Hofweber[2,3], Gesa Richter[1], Julia Sternat[1], Claudia Abou-Ajram[2], Christoph Göbl[1], Gerd Leitinger[4], Wolfgang F. Graier[1,5], Dorothee Dormann[2,3,6,*], Tobias Madl[1,5,*]

[1]Gottfried Schatz Research Center for Cell Signaling, Metabolism and Aging, Molecular Biology & Biochemistry, Medical University of Graz, 8010 Graz, Austria.
[2]BioMedical Center (BMC), Cell Biology, Ludwig-Maximilians-University Munich, 82152 Planegg-Martinsried, Germany.
[3]Graduate School of Systemic Neurosciences (GSN); 82152 Planegg-Martinsried, Germany.
[4]Gottfried Schatz Research Center for Cell Signaling, Metabolism and Aging, Division of Cell Biology, Histology and Embryology, Medical University of Graz, 8010 Graz, Austria.
[5]BioTechMed-Graz, 8010 Graz, Austria.
[6]Munich Cluster for Systems Neurology (SyNergy); 81377 Munich, Germany.

***Correspondence should be addressed to:**

Tobias Madl (lead contact)
Phone: (+43-316) 385-71972
Fax: (+43-316) 385-79615
E-Mail: tobias.madl@medunigraz.at

or

Dorothee Dormann
Phone: (+49-89) 2180-75876
Fax: (+49-89) 2180-75882
E-Mail: dorothee.dormann@med.uni-muenchen.de

† Equal contribution

This PDF file includes:

Supplementary text
Figures S1 to S6
Legends for Movies S1 to S2
Legends for Datasets S1 to S2
SI References

Other supplementary materials for this manuscript include the following:

Movies S1 to S2
Datasets S1 to S2

SI Material and methods

Plasmids

To generate GST-GFP-CIRBP, full length human-CIRBP was PCR amplified (primer sequences: agactcgagctatggcatcagatgaaggcaaac; aatggatccttactcgttgtgtgtagcgtaactgtcataac) and inserted into a pEGFP-C1 vector (Clontech) containing a GST-GFP cassette (1) via XhoI and BamHI restriction digest. To generate GCR_2-$EGFP_2$-CIRBP full length and deletion constructs, the NLS sequence in a modified pEGFP-C1 vector containing a GCR_2-$EGFP_2$-cassette (2) was replaced by either full length CIRBP or cDNAs lacking the RRM (aa 1-67), RG/RGG (aa 91-137), RSY (138-172) or RG/RGG-RSY (aa 91-172) domains using EcoRV and BamHI.
Expression constructs for the fragments of human CIRBP from amino acid 1 to 90 ($CIRBP^{RRM}$), amino acid 68 to 137 ($CIRBP^{RGG}$), amino acid 138 to 172 wild type, R to A mutant, Y to A mutant ($CIRBP^{RSY}$, $CIRBP^{ASY}$ and $CIRBP^{RSA}$, respectively), and amino acid 1 to 172 (full-length CIRBP) were generated by synthesis of the corresponding optimized CIRBP cDNA constructs (Genscript) and insertion of these cDNA into pETM11-ZZ-His_6 vector via NcoI/BamHI restriction digest. We also generated optimized cDNA expression constructs (Genscript) in pETM11-ZZ-His_6 vector for fragments of human TNPO1 from amino acids 328 to 381 ($TNPO1^{loop}$), amino acids 1 to 898 depleted from amino-acids 328 to 381 ($TNPO1^{\Delta loop}$) and amino-acids 1 to 898 (TNPO1) and human TNPO3 full length. The expression construct for the fragment of human FUS from amino acid 504 to 526 (FUS^{PY}) in pETM11-ZZ-His_6 vector was previously described in (3).The expression construct for the fragment of rat PRMT1 in pET28b-His_6 vector from amino acids 11 to 353 was previously described in (4)

Protein expression and purification

For expression of recombinant unlabeled or ^{15}N labeled or ^{15}N-^{13}C labeled ZZ- His_6 proteins, the different bacterial expression pETM11-ZZ-His_6 vectors were transformed into *Escherichia coli (E.coli)*BL21-DE3 Star strain and 1 L expression cultures were grown for 2 days in minimal medium supplemented with either 6 g of $^{12}C_6H_{12}O_6$ or 2 g of $^{13}C_6H_{12}O_6$ (Cambridge Isotope Laboratories) and either 3 g of $^{14}NH_4Cl$ or $^{15}NH_4Cl$ (Sigma). Cells were diluted to an OD (600nm) of 0,8 and induced with 0.5 mM IPTG followed by protein expression for 4 h at room temperature ($CIRBP^{RSY}$, $CIRBP^{ASY}$, $CIRBP^{RSA}$, $TNPO1^{loop}$, $TNPO1^{\Delta loop}$, TNPO1, FUS^{PY}) or 16 h at 20°C ($CIRBP^{RRM}$, $CIRBP^{RGG}$, TNPO3) or 2 h at 37°C (full-length CIRBP). For expression of perdeuterated [U-^{2}H,^{13}C,^{15}N,IM-methyl ^{1}H,^{13}C] TNPO1, 50mg of 2-Ketobutyric acid 4-13C (Sigma) and 50mg of L-methionine-methyl-13C (Cambridge Isotope Laboratories) was added before induction using 99% deuterated minimal medium. For expression of recombinant unlabeled His_6 -PRMT1, the pET28b-His_6-PRMT1 was transformed into *E.coli* BL21-DE3 Star strain and 1 L expression culture was grown in lysogeny broth (LB) medium. Cells were induced at an OD (600nm) of 0,8 with 0.5 mM IPTG followed by protein expression for 16 h at 20°C. Cells pellets corresponding for protein expression of unlabeled or ^{15}N labeled or ^{15}N-^{13}C labeled disordered proteins fragments ($CIRBP^{RGG}$, $CIRBP^{RSY}$, $CIRBP^{RSA}$, $CIRBP^{RSY}$, FUS^{PY} and $TNPO1^{loop}$) were harvested and sonicated in denaturating lysis buffer (50 mM Tris-HCl pH 7.5, 150mM NaCl, 20 mM Imidazole,

6M urea) whereas the folded proteins fragments (CIRBP^{RRM}, TNPO1$^{\Delta loop}$, TNPO1, TNPO3 and PRMT1) were harvested and sonicated in non denaturating lysis buffer (50mM Tris-HCl pH 7.5, 150mM NaCl, 20mM Imidazole, 2mM tris(2-carboxyethyl)phosphine) .For CIRBP^{RRM} and full-length CIRBP, cell lysates were incubated for 30 min at room temperature with RNase A (Life Technologie) before centrifugation. ZZ-His_6 or His_6 recombinant proteins were then purified using Ni-NTA agarose beads (Quiagen) and the ZZ-His6 tag was cleaved with TEV protease treatment. Untagged proteins were then isolated performing a second affinity purification using Ni-NTA beads. A final exclusion chromatography purification step was performed in the buffer of interest on a gel filtration column (Superdex 200, GE Healthcare for TNPO1$^{\Delta loop}$, TNPO1, TNPO3 and PRMT1; Superdex 75 GE Healthcare for CIRBP^{RRM} and full-length CIRBP; and Superdex peptide, GE Healthcare for CIRBP^{RSY}, CIRBP^{ASY}, CIRBP^{RSA}, CIRBP^{RGG}, FUS^{PY} and TNPO1^{loop}). Protein concentrations were estimated from their absorbance at 280 nm, assuming that the ε at 280 nm was equal to the theoretical ε value.

cDNA and siRNA transfection

cDNA transfections of GST-GFP- and GCR_2-GFP_2-CIRBP reporters into HeLa Kyoto were performed using either Lipofectamine 2000 or Turbofect (Thermo Fisher Sc.) and cells fixed for analysis on the following day. As control for free diffusion of the reporter protein (100kDa), a construct with a stop codon downstream of the GCR_2-GFP_2- fusion was used (GCR_2-GFP_2-stop-M9).
For analysis of cellular localization of GST-GFP-CIRBP in HeLa Kyoto cells upon siRNA treatment, HeLa Kyoto cells were transfected using 20 nM non-targeting control siRNA (siNTC, Invitrogen) or siTNPO3 (Qiagen; #si00100513 AND si00100534; target sequence: ACCGAATGTCTTAGTGAACTA and CAAGTGGTCATGGGTATCTTA, respectively) or 5 nM of siTNPO1 (Ambion Silencer® Select, siRNA ID #s7933 (sense: GCCGUUGCAUCAUGGAUUAtt; antisense: UAAUCCAUGAUGCAACGGCat) and #s7932 (sense: GGAACAACUUAAUCAGUAUtt; antisense: AUACUGAUUAAGUUGUUCCag)) using RNAiMaxx (Invitrogen).
Cells were transferred onto 12 mm high precision coverslips (No. 1.5) at day 1 after siRNA transfection. Reporter constructs were transfected at day 2 after siRNA transfection and cells analyzed the following day. Efficiency of KD was analyzed by western blotting using antibodies specific for TNPO1 (Sigma; clone D45; #T 0825) and TNPO3 (abcam; clone 3152C2a, #ab54353). Blotting against GAPDH (clone 4H11, gift from E. Kremmer) served as loading control.
For localization assays in HeLa S3cells, cells were transfected at 50 % confluency in DMEM (without FCS and antibiotics) with 1.5 µg/ml plasmid of GST-GFP-CIRBP and 100 nM of control (5'-UUCUCCGAACGUGUCACGU-3') or PRMT1 (5'-CGUCAAACCCAACAAGUUAdTdT-3') siRNA (Microsynth) with 2,5 µg/ml TransFast^{TM} transfection reagent (Promega). 40 µM adenosine dialdehyde (ADOX, Sigma Aldrich) was added 2 h post transfection. After 24h, the medium was replaced with DMEM with or without 40µM ADOX containing 10% FCS and penicillin and streptomycin and kept for further 24 h prior to experiments.

Microscopy

Widefield microscopy

For localization analysis of GST-GFP-CIRBP in live HeLa S3 cells, cells were incubated with 5 µg/ml bisBenzimide H 33342 trihydrochloride (14533, Sigma) in loading buffer containing 135mM NaCl, 5mM KCl, 2mM $CaCl_2$, 1mM $MgCl_2$, 10mM Hepes, 2.6mM $NaHCO_3$, 440 mM KH_2PO_4, 340 mM Na_2HPO_4, 10mM D-glucose, 0.1% vitamins, 0.2% essential amino acids, and 1% penicillin–streptomycin, pH adjusted to 7.4 for 20 min and washed twice afterwards with loading buffer before imaging. Cells were imaged in imaging buffer containing $CaCl_2$, 140 NaCl, 5 KCl, 1 $MgCl_2$, 1 HEPES and 10 D-Glucose, pH adjusted to 7.4 (all buffer salts were obtained from Roth, Graz, Austria) with a CFI Super Fluor 40X Oil 1.30 NA objective mounted on a Nikon Eclipse Ti system with standard Nikon wide field filter sets and equipped with two Andor iXon3® EMCCD camera mounted to a Two Camera Imaging Adapter (Nikon Austria, Vienna, Austria). A Polychrome V monochromator (Till

Photonics) was used for illumination. Hoechst 33342 was illuminated at 380 nm and the GST-GFP-CIRBP with 488 nm wavelength.

Confocal microscopy

Confocal microscopy was performed at the Bioimaging core facility of the Biomedical Center with an inverted Leica SP8 microscope, equipped with lasers for 405, 488, 552 and 638 nm excitation. Images were acquired using two-fold frame averaging with a 63x1.4 oil objective, and an image pixel size of 59 nm. The following fluorescence settings were used for detection: DAPI: 419-442 nm, GFP: 498-533 nm. Recording was performed sequentially to avoid bleed-through using a conventional photomultiplier tube.

Live Cell Imaging of CIRBP Import

To illustrate the import of full length CIRBP by live cell imaging, HeLa Kyoto cells were grown in a 4-well live cell imaging dish (ibidi) and transiently transfected with GCR_2-GFP_2-stop-M9 or –CIRP fl.. Live cell imaging was performed on the following day at 36.5°C/5% CO_2 in a culture medium lacking phenol red (Fluorobrite; Thermo Fisher Sc.) on an inverted microscope (Axio Observer.Z1; Carl Zeiss, Oberkochen, Germany) equipped with a confocal spinning disk unit (CSU-X1; Yokogawa, Tokyo, Japan) and a Zeiss 63x/1.4 Oil oil immersion lens. Import of the GCR_2-GFP_2-reporter was induced by addition of dexamethasone (final 5µM) to the medium directly after the acquisition of the first frame. Images were acquired using the 488 nm SD laser line in intervals of 2.5 min and an EM-CCD camera (EvolveDelta; Photomoetrics) at bin 1x1.

***In vitro* methylation assay**

NMR analysis of *in vitro* PRMT1-methylated CIRBP using ^{1}H-^{15}N-^{13}C (H)CC(CO)NH experiment. Methylated arginines show a carbon delta (Cδ) resonance shifted by about 2 ppm compared to unmethylated arginines. This allowed us to cluster arginines in CIRBP depending on their degree of methylation in 4 groups: (a) unmethylated arginines (R75, 78, 89, 127 and 131), (b) mainly unmethylated arginines (R91 and 121), (c) mainly methylated arginines (R94) (d) methylated arginines (R101 and 105) (Figure S5A). Given overlapping NMR signals on the ^{1}H, ^{15}N, ^{13}C (H)CC(CO)NH corresponding to the R108, 110, 112 and 116 we cannot access residue-specific methylation status for these arginines, nevertheless the corresponding NMR signal match with mainly methylated arginines.

SI Figure legends

Fig. S1.

(A) Cellular redistribution of a reporter lacking a NLS (GCR_2-GFP_2-stop-M9) over time upon addition of dexamethasone visualized by live cell imaging in HeLa Kyoto cells. Bar, 20 µm. (B) Quantification related to figure 1D of the subcellular localization of the individual reporter proteins (N>C, N=C and N<C). Values represent mean of 5 independent experiments ±SEM for CIRBP constructs, and 2 independent experiments for the stop-construct (control for free diffusion), *** p<0.001; ** p<0.01; * p<0.05 by 2-way ANOVA+Bonferroni multiple comparison test; only significant comparisons are shown. (C) Western Blot demonstrating the knockdown (KD) efficiency by siRNA treatment using specific antibodies for TNPO1 and TNPO3, respectively. GAPDH serves as loading control. Note that lysate derived from siNTC transfected cells was titrated (100%, 25%) to allow for a better estimation of KD efficiency. (D) Quantification related to figure 1E of the subcellular localization of the individual reporter proteins (N>C, N=C and N<C). Values represent mean of 3 independent experiments ±SEM, *** p<0.001; ** p<0.01; * p<0.05 by 2-way ANOVA+Bonferroni multiple comparison test.

Fig. S2.

(A) PONDR score of CIRBP^{FL} using the VSL2 predictor (http://www.pondr.com) (B) Association of MBP-CIRBP-EGFP with SGs in semi-permeabilized cells is suppressed by TNPO1 or TNPO3 in a concentration dependent manner. Bar, 10 µm. (C) Quantification of the mean fluorescence intensity of MBP-CIRBP-EGFP in SGs in the absence of presence of increasing concentrations of either TNPO1 or TNPO3 for four or two (2 µM TNPO3) independent replicates with ≥28 SGs ± SEM. **p<0.01 and ***p<0.001 by 1-way ANOVA Dunett's multiple comparison test (D) Turbidity assay to quantify phase separation of different CIRBP constructs with increasing CIRBP concentration (E) DIC microscopy images of different CIRBP constructs using CIRBP at 30µM and/or in presence of 10 µM RNA and/or 30 µM TNPO1 or -3. Scale bar, 10 µm. (F, G) Turbidity assay to quantify phase separation of CIRBP^{RGG} with fixed CIRBP concentration (30 µM) and increasing RNA concentration in (F), with fixed CIRBP and RNA concentration (30 µM and 10 µM, respectively) and increasing TNPO1 or TNPO3 concentration in (G) (black and red lines, respectively). Values represent means ± SEM (n=3). (H) Overlay of ^{1}H-^{15}N HSQC NMR spectra of 30 µM ^{15}N-labeled CIRBP^{RGG} (bleu), in presence of 10 µM RNA (red), and with increasing amount of TNPO1 (orange, left panel), or TNPO3 (yellow, right panel). The reference ^{1}H-^{15}N HSQC NMR spectra of ^{15}N-labeled CIRBP^{RGG} with TNPO1 or 3 (green, right panel and cyan, left panel, respectively) are also shown.

Fig. S3.

(A) *Left panel*: Titration of 100 µM CIRBP^{FL} into 10 µM of TNPO1. The resulting Kd yielded 741 ± 106 nM. The reported errors correspond to the SD of the fit. *Right panel*: Titration of 100 µM CIRBP-FL into 10 µM of TNPO3. The resulting Kd yielded 289 ± 36 nM. The reported errors correspond to the SD of the fit. (B) *Left panel:* Titration of 100 µM CIRBP^{RGG} into 10 µM of TNPO1. The resulting Kd yielded 75 ± 13 nM. The reported errors correspond to the SD of the fit. *Right panel:* Titration of 300 µM CIRBP^{RSY} into 30 µM of TNPO1. The resulting Kd yielded 7800 ± 545 nM. The reported errors correspond to the SD of the fit. (C) *Left panel:* Titration of 100 µM CIRBP^{RGG} into 10 µM of TNPO3. The resulting Kd yielded 589 ± 70 nM. The reported errors correspond to the SD of the fit. *Right pane*l: Titration of 100 µM CIRBP^{RSY} into 10 µM of TNPO3. The resulting Kd yielded 114 ± 5 nM. The reported errors correspond to the SD of the fit. (D) ^{1}H-^{15}N HSQC spectrum of ^{15}N-labeled CIRBP^{RRM} at 50 µM without (cyan) or with addition of 1 equivalent of TNPO1 (bleu, left panel) or TNPO3 (black, right panel). (E) ^{1}H-^{15}N HSQC spectrum of ^{15}N-labeled mutant CIRBP^{RSA} at 50 µM without (red) or with addition of 1 equivalent of TNPO1 (bleu, left panel) or TNPO3 (black, right panel). (F) ^{1}H-^{15}N HSQC spectrum of ^{15}N-labeled mutant CIRBP^{ASY} at 50 µM without (red) or with addition of 1 equivalent of TNPO1 (bleu, left panel) or TNPO3 (black, right panel). (G) ^{1}H projection of the ^{1}H-^{15}N HSQC spectrum of ^{15}N-labeled CIRBP^{RGG} at 50 µM, unbound (black, dotted line), bound to 1 equivalent of TNPO1 or -3 (light grey, left and right panel respectively), plus 1 or 2 equivalent of Ran-GTP (grey and dark grey, respectively). (H) ^{1}H projection of the ^{1}H-^{15}N HSQC spectrum of ^{15}N-labeled CIRBP^{RSY} at 50 µM, unbound (black, dotted line), bound to 1 equivalent of TNPO1 or -3 (light grey, left and right panel respectively), plus 1 or 2 equivalent of Ran-GTP (grey and dark grey, respectively). (I) ^{1}H-^{15}N HSQC spectrum of ^{15}N-labeled FUS^{PY} at 50 µM without (black) or with addition of 1 equivalent of TNPO3 (magenta, left panel)

Fig. S4.

(A) *Left panel:* Titration of 100 µM CIRBP^{RGG} into a solution containing 10 µM of TNPO1 pre-equilibrated with 50 µM of FUS^{PY}. The resulting Kd yielded 391 ± 77 nM. The reported errors correspond to the SD of the fit. *Middle panel:* Titration of 100 µM FUS^{PY} into a solution containing 7.5 µM of TNPO1 pre-equilibrated with 50 µM of CIRBP^{RGG}. The resulting Kd yielded 413 ± 41 nM. The reported errors correspond to the SD of the fit. *Right panel*: Titration of 100 µM FUS^{PY} into 10 µM of TNPO1. The resulting Kd yielded 48 ± 6 nM. The reported errors correspond to the SD of the fit. (B) ^{1}H-^{15}N HSQC spectrum of ^{15}N-labeled TNPO1^{loop} at 50 µM without (blue) or with addition of either 1 equivalent of FUS^{PY} (magenta, left panel) or CIRBP-RSY (red, right panel). (C) Titration curve corresponding to experiment in (Fig. 4C) with increasing amount of CIRBP^{RGG}. The ^{1}H-^{15}N combined chemical shift perturbations (CSP) is plotted as a function of the CIRBP^{RGG}

concentration. Dissociation constants (K_d) were obtained by nonlinear regression based on a single binding site model. (D) *Left panel*: Titration of 100 µM CIRBP^{RGG} into 10 µM of TNPO1$^{\Delta loop}$. The resulting Kd yielded 364 ± 15 nM. The reported errors correspond to the SD of the fit. *Middle panel:* Titration of 380 µM CIRBP^{RSY} into 30 µM of TNPO1Δloop. The resulting Kd yielded 8075 ± 566 nM. The reported errors correspond to the SD of the fit. *Right panel:* Titration of 100 µM FUS^{PY} into 10 µM of TNPO1$^{\Delta loop}$. The resulting Kd yielded 62 ± 4 nM. The reported errors correspond to the SD of the fit.

Fig. S5.

(A) *upper panel:* Schematic representation of the RG/RGG region of CIRBP. The PRMT1-mediated methylated arginine derived from NMR analysis are colored in red. *Downer panel:* ^{1}H-^{15}N-^{13}C (H)CC(CO)NH spectrum of PRMT1-mediated methylated CIRBP^{RGG}. The region corresponding to the Cδ of arginines is zoomed. (B) *Left panel:* Titration of 100 µM PRMT1-mediated methylated-CIRBP^{RGG} (meCIRBP^{RGG}) into 10 µM of TNPO1. No detectable binding. *Right panel:* Titration of 100 µM PRMT1-mediated methylated-CIRBP full-length (meCIRBP) into 10 µM of TNPO1. No detectable binding. (C) *Left panel:* Titration of 130 µM PRMT1-mediated methylated-CIRBP^{RGG} (meCIRBP^{RGG}) into 10 µM of TNPO3. The resulting Kd yielded 3300 ± 320 nM. The reported errors correspond to the SD of the fit. *Right panel:* Titration of 80 µM PRMT1-mediated methylated-CIRBP full-length (meCIRBP) into 10 µM of TNPO3. The resulting Kd yielded 1002 ± 100 nM. The reported errors correspond to the SD of the fit. (D) Reduced interaction of TNPO1 and TNPO3 from HeLa cell lysate with methylated CIRBP. Unmethylated (unme) and methylated (me) His6-ZZ-CIRBP was immobilized on Ni-NTA beads and incubated with total HeLa cell lysate. Empty beads were included as control for background binding. TNPO1 and TNPO3 bound to unmethylated and methylated His6-ZZ-CIRBP were detected by Western Blot using specific antibodies. Equal immobilization of unmethylated and methylated His6-ZZ-CIRBP is demonstrated with a His6-specific antibody. The normalized intensity (unme set to 100%) of TNPO1 (left) and TNPO3 (right) binding to CIRBP is shown on the right. Values represent means ± SEM (n=3), **p<0.01 by unpaired, two-tailed t-test.

Fig. S6.

(A) BLASTp analysis of the RSY region of CIRBP against the non-redundant protein sequences database filtered for human proteins (taxid:9606). The obtained protein sequences *(upper panel)* and their architectural organization are shown *(downer panel)*.

Movie S1 (separate file).

Movie illustrating time dependent nuclear localization of a reporter lacking a NLS (stop-M9) due to passive diffusion corresponding to montages in figure S1A. Bar, 20µm.

Movie S2 (separate file).

Movie illustrating time dependent nuclear import of CIRBP-FL corresponding to montages in figure 1B. Bar, 20µm.

Dataset S1 (separate file).

List of proteins corresponding to the PROSITE analysis (https://prosite.expasy.org/scanprosite/) of two motifs against the non-redundant protein sequences database filtered for human proteins (taxid:9606) harboring either (i) a di-RG motif each spaced by 0 to 5 amino-acids (R-G-x(0-5)-R-G) (ii) a PY motif bpreceded by a basic amino-acid spaced by 0 to 9 residues ([RKH]-x(0,9)-P-Y) (iii) both motifs

Dataset S2 (separate file).

List of proteins corresponding to the PROSITE analysis (https://prosite.expasy.org/scanprosite/) of two motifs against the non-redundant protein sequences database filtered for human proteins

(taxid:9606) harboring both a di-RG motif each spaced by 0 to 5 amino-acids (R-G-x(0-5)-R-G) and a tri-RS or SR motif.

SI References

1. D. Dormann *et al.*, ALS-associated fused in sarcoma (FUS) mutations disrupt Transportin-mediated nuclear import. *The EMBO journal* **29**, 2841-2857 (2010).
2. S. Hutten, A. Flotho, F. Melchior, R. H. Kehlenbach, The Nup358-RanGAP complex is required for efficient importin alpha/beta-dependent nuclear import. *Molecular biology of the cell* **19**, 2300-2310 (2008).
3. D. Dormann *et al.*, Arginine methylation next to the PY-NLS modulates Transportin binding and nuclear import of FUS. *The EMBO journal* **31**, 4258-4275 (2012).
4. X. Zhang, X. Cheng, Structure of the predominant protein arginine methyltransferase PRMT1 and analysis of its binding to substrate peptides. *Structure* **11**, 509-520 (2003).

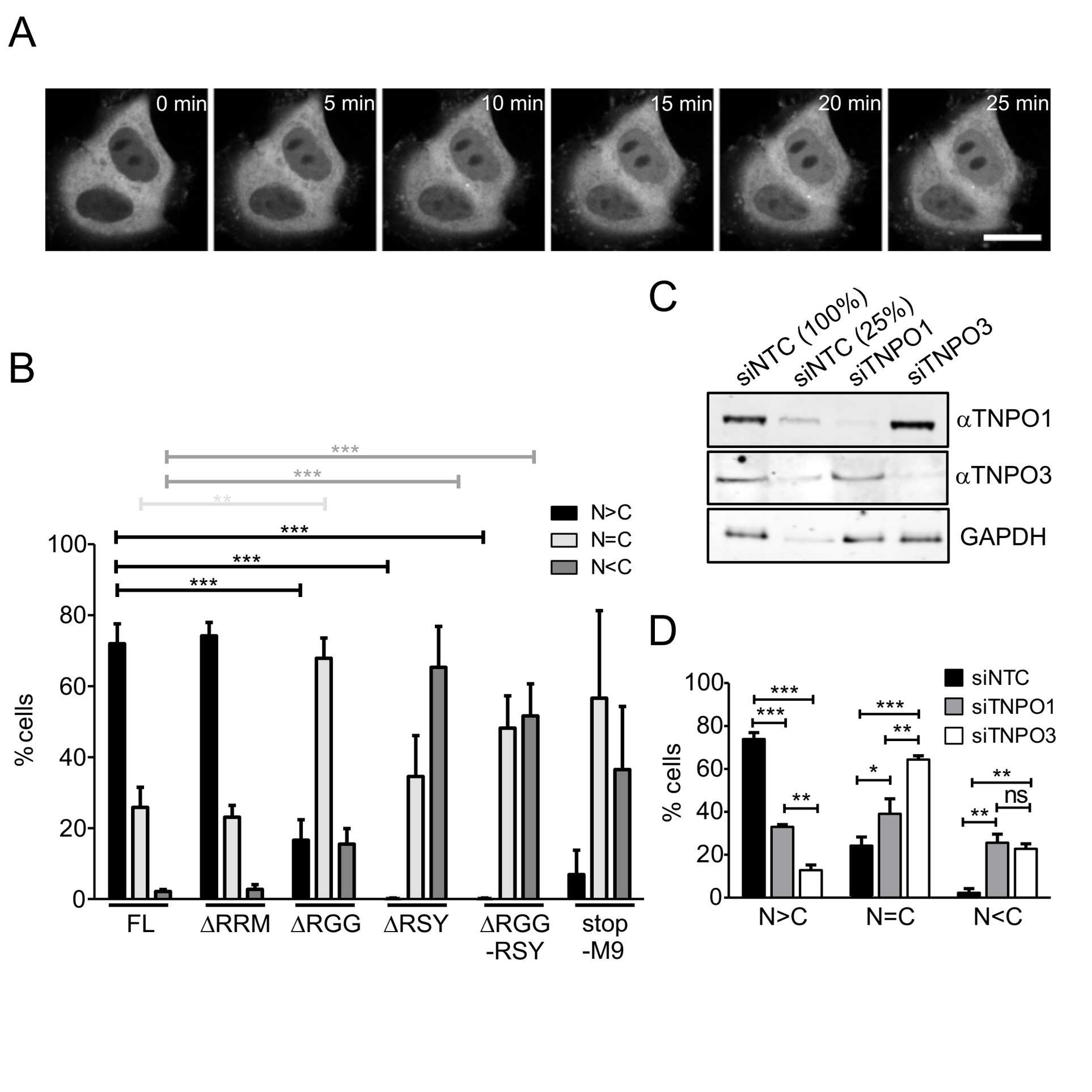
A
0 min
5 min
10 min
15 min
20 min
25 min
B
N>C
N=C
N<C
% cells
FL
ΔRRM
ΔRGG
ΔRSY
ΔRGG -RSY
stop -M9
C
siNTC (100%)
siNTC (25%)
siTNPO1
siTNPO3
αTNPO1
αTNPO3
GAPDH
D
siNTC
siTNPO1
siTNPO3
% cells
N>C
N=C
N<C
ns

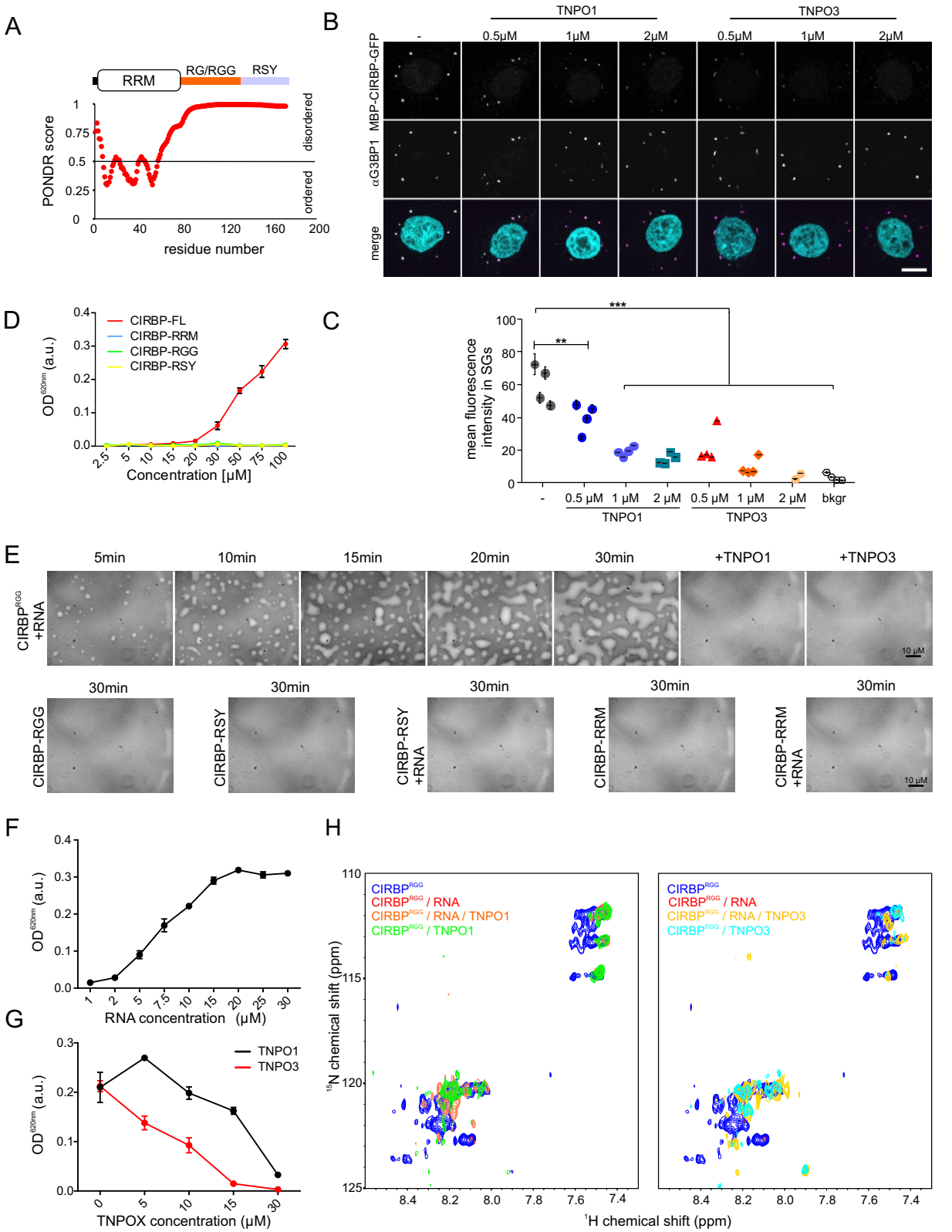
A
RRM
RG/RGG
RSY
PONDR score
disordered
ordered
residue number
B
TNPO1
TNPO3
-
0.5μM
1μM
2μM
0.5μM
1μM
2μM
MBP-CIRBP-GFP
αG3BP1
merge
C
mean fluorescence intensity in SGs
***
**
- 0.5 μM 1 μM 2 μM 0.5 μM 1 μM 2 μM bkgr
TNPO1
TNPO3
D
CIRBP-FL
CIRBP-RRM
CIRBP-RGG
CIRBP-RSY
OD620nm (a.u.)
Concentration [μM]
E
5min
10min
15min
20min
30min
+TNPO1
+TNPO3
CIRBPRGG +RNA
10 μM
30min
CIRBP-RGG
CIRBP-RSY
CIRBP-RSY +RNA
CIRBP-RRM
CIRBP-RRM +RNA
F
OD620nm (a.u.)
RNA concentration (μM)
G
TNPO1
TNPO3
OD620nm (a.u.)
TNPOX concentration (μM)
H
CIRBPRGG
CIRBPRGG / RNA
CIRBPRGG / RNA / TNPO1
CIRBPRGG / TNPO1
CIRBPRGG / RNA / TNPO3
CIRBPRGG / TNPO3
15N chemical shift (ppm)
1H chemical shift (ppm)

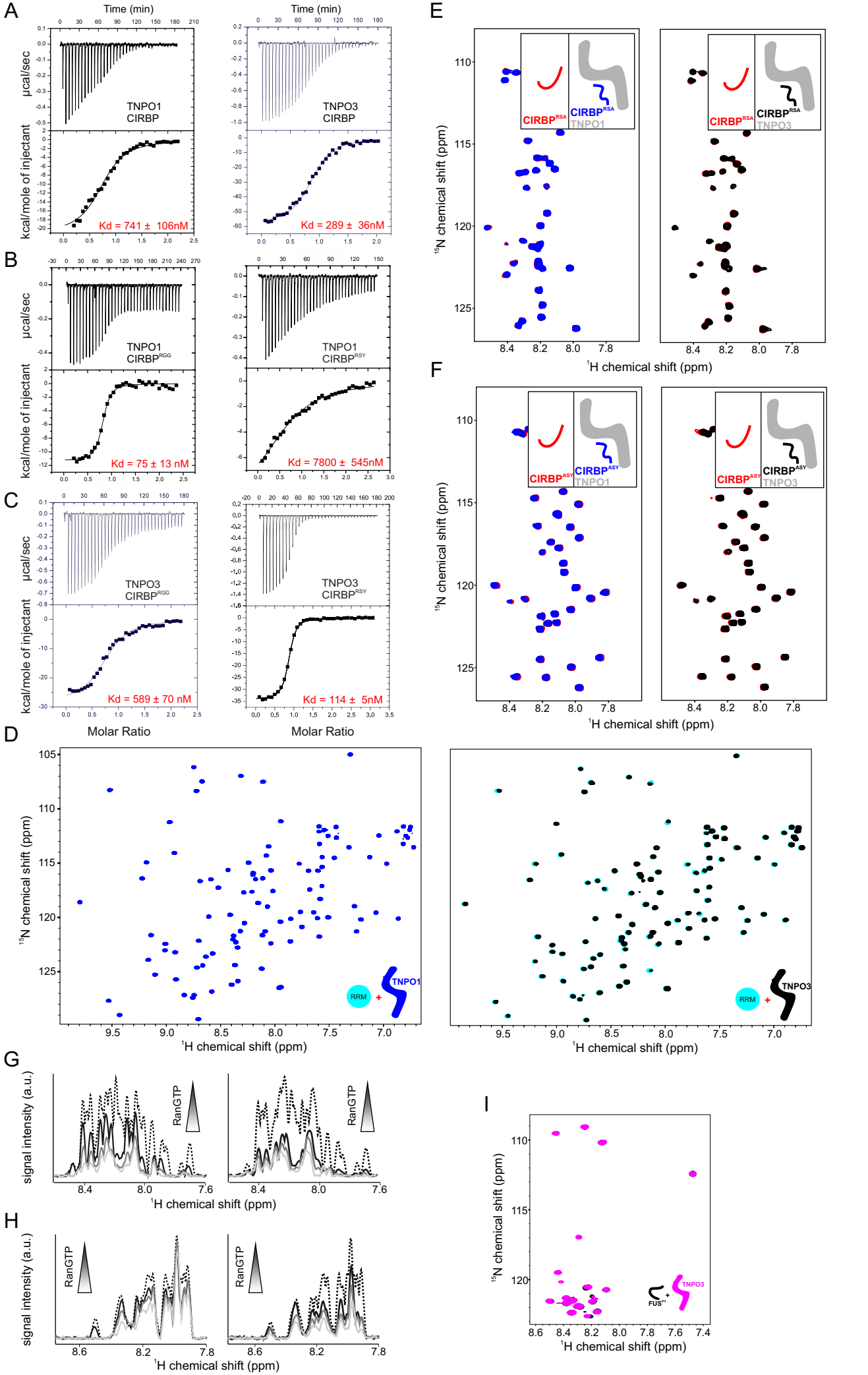
A
Time (min)
µcal/sec
kcal/mole of injectant
TNPO1
CIRBP
Kd = 741 ± 106nM
TNPO3
CIRBP
Kd = 289 ± 36nM
B
TNPO1
CIRBP^RGG
Kd = 75 ± 13 nM
TNPO1
CIRBP^RSY
Kd = 7800 ± 545nM
C
TNPO3
CIRBP^RGG
Kd = 589 ± 70 nM
TNPO3
CIRBP^RSY
Kd = 114 ± 5nM
Molar Ratio
D
15N chemical shift (ppm)
1H chemical shift (ppm)
RRM
TNPO1
TNPO3
E
CIRBP^RSA
CIRBP^RSA
TNPO1
TNPO3
F
CIRBP^ASY
CIRBP^ASY
TNPO1
TNPO3
G
signal intensity (a.u.)
RanGTP
H
I
FUS^PY
TNPO3

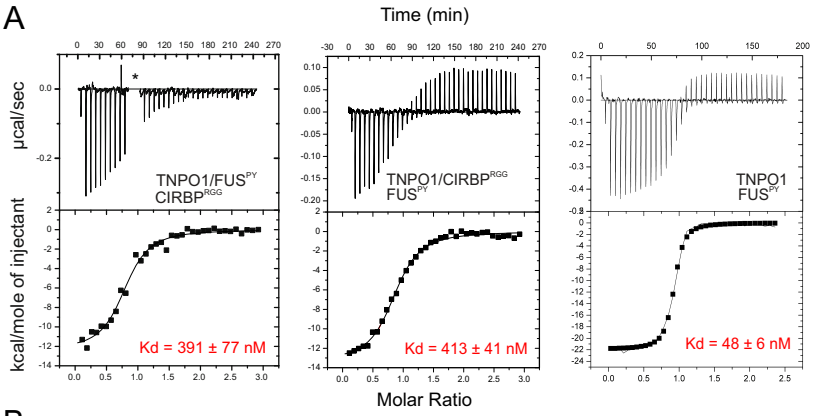
A
Time (min)
µcal/sec
kcal/mole of injectant
TNPO1/FUS^PY
CIRBP^RGG
Kd = 391 ± 77 nM
TNPO1/CIRBP^RGG
FUS^PY
Kd = 413 ± 41 nM
TNPO1
FUS^PY
Kd = 48 ± 6 nM
Molar Ratio

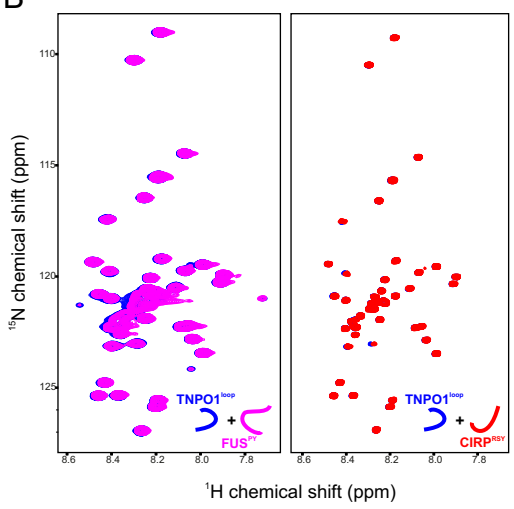
B
15N chemical shift (ppm)
TNPO1^loop
FUS^PY
TNPO1^loop
CIRP^RSY
1H chemical shift (ppm)

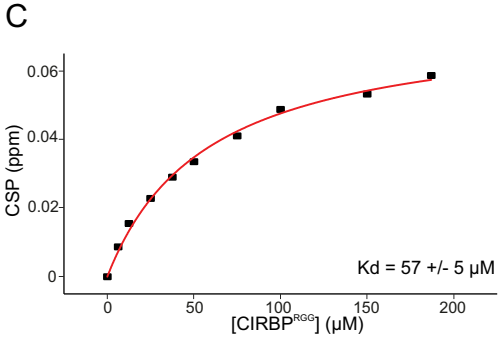
C
CSP (ppm)
Kd = 57 +/- 5 µM
[CIRBP^RGG] (µM)

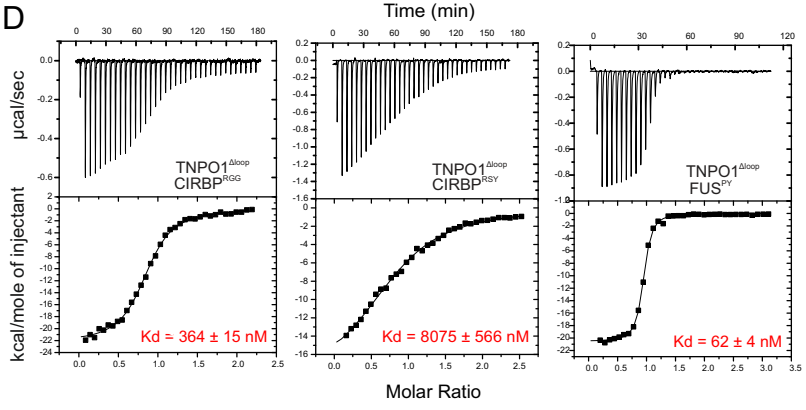
D
Time (min)
µcal/sec
kcal/mole of injectant
TNPO1^Δloop
CIRBP^RGG
Kd = 364 ± 15 nM
TNPO1^Δloop
CIRBP^RSY
Kd = 8075 ± 566 nM
TNPO1^Δloop
FUS^PY
Kd = 62 ± 4 nM
Molar Ratio

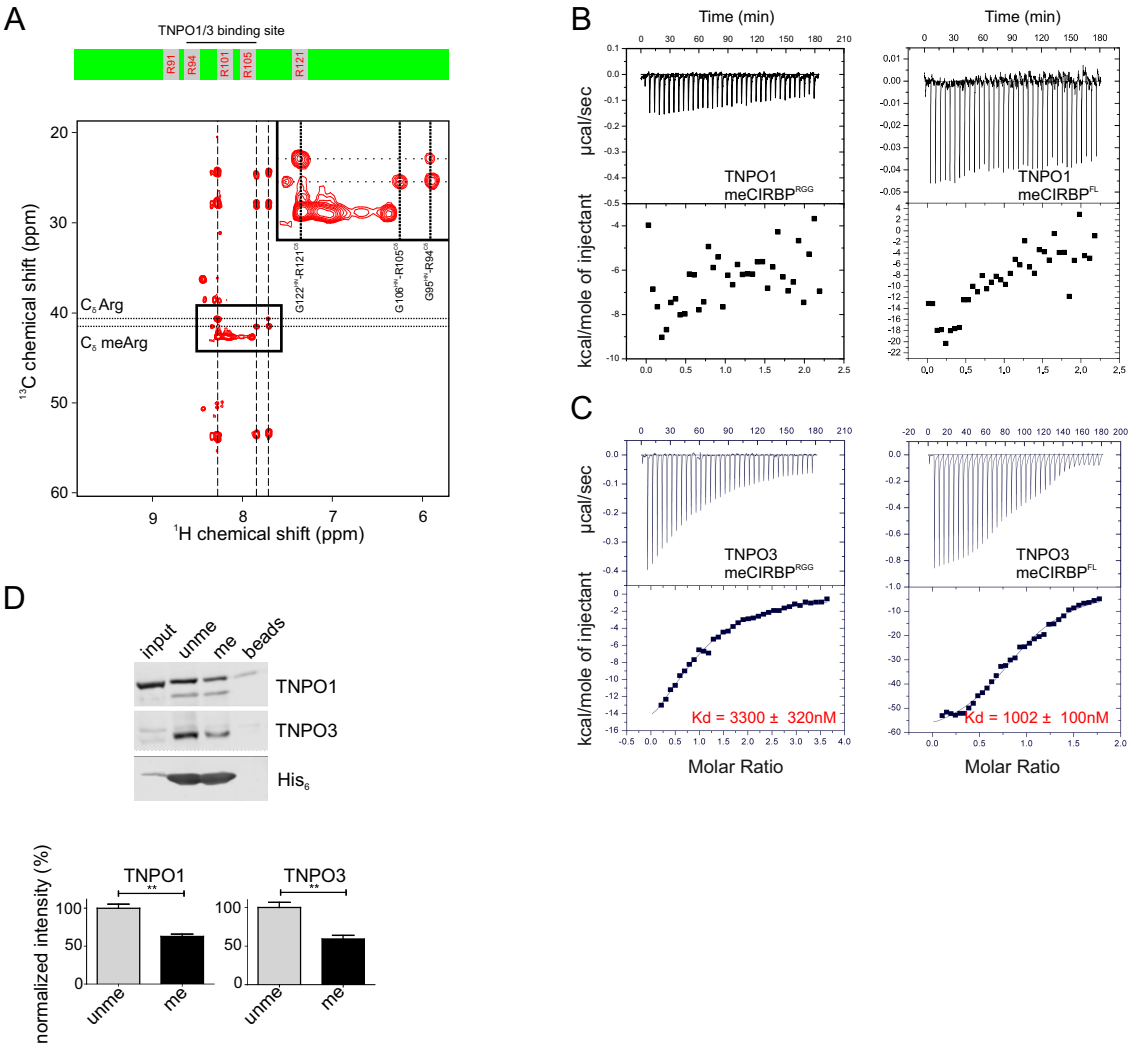
A
TNPO1/3 binding site
R91
R94
R101
R105
R121
^{13}C chemical shift (ppm)
^{1}H chemical shift (ppm)
C_δ Arg
C_δ meArg
G122^{HN}-R121^{CO}
G106^{HN}-R105^{CO}
G95^{HN}-R94^{CO}
B
Time (min)
µcal/sec
kcal/mole of injectant
TNPO1
meCIRBP^{RGG}
TNPO1
meCIRBP^{FL}
C
TNPO3
meCIRBP^{RGG}
TNPO3
meCIRBP^{FL}
Kd = 3300 ± 320nM
Kd = 1002 ± 100nM
Molar Ratio
D
input
unme
me
beads
TNPO1
TNPO3
His$_6$
normalized intensity (%)
TNPO1
TNPO3
**
unme
me

A

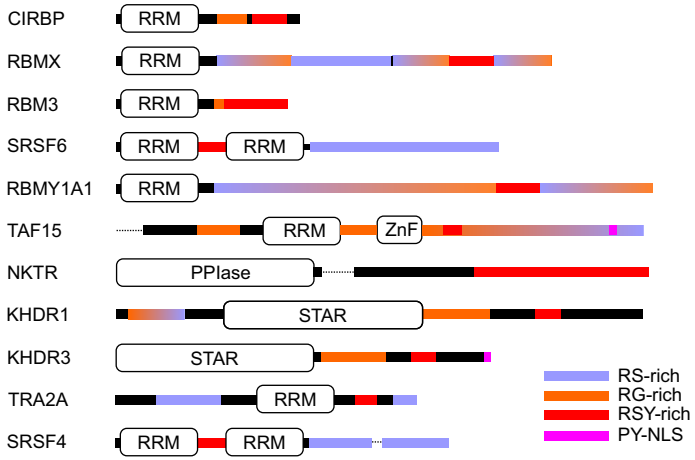

CIRBP 138 SRDYYSSRSQSGGYSDRSSGGSYRDSYDSYATHNE 172

RBMX 312 DYSSSRDGYGGSRDSYSS 329

RBM3 135 YNGRNQGGYDRYSGGNYRDNYD 156

SRSF6 82 YGSRSGGGGYSSRRTSGRDKY 102

RBMY1A1 363 SSRGYS...SGSYRDALQRYGT 399

TAF15 422 RSGGGYGGDRSSGGGY 437

NKTR 1407YYSRSRSRSRSQRSDSYHRGRSY 1429

KHDR1 386 YYSQSQGDSEYYDYGHGEVQDSY 408

KHDR3 270 DYDDGYGTAYDEQSYDSY 287

TRA2A 234 RDSYYDRGYDRGYDRYEDYDYR 255

SRSF4 75 RDGSYGSGRSGYGYRRSGRD 94